Sensors and Materials, Vol. 38, No. 2 (2026) 565–570
MYU Tokyo

S & M 4322

Optical and Scintillation Properties of Tm-doped Y_2O_3 Transparent Ceramics Synthesized by the Spark Plasma Sintering Method

Yuma Saito,* Shota Otake, Takumi Kato,
Daisuke Nakauchi, Noriaki Kawaguchi, and Takayuki Yanagida

Nara Institute of Science and Technology (NAIST), 8916-5 Takayama-cho, Ikoma-shi, Nara 630-0192, Japan

(Received October 21, 2025; accepted December 16, 2025)

Keywords: scintillator, phosphor, transparent ceramic, SPS, Y_2O_3

Tm:Y_2O_3 transparent ceramic scintillators with Tm concentrations of 0.01, 0.1, 1.0, and 10 mol% were fabricated by the spark plasma sintering method to investigate their photoluminescence (PL) and scintillation properties. Both PL and scintillation peaks were observed in the range of 350–650 nm, corresponding to the 4f–4f transitions of Tm^{3+}. Scintillation decay curves were well-approximated by two exponential components with decay time constants of 1.8–6.9 and 10–40 μs. Afterglow levels ranged from approximately 250 to 800 ppm and tended to decrease with Tm concentration. Scintillation light yields under ^{241}Am α-ray (5.5 MeV) irradiation were estimated to be approximately 1400–1500 photons/5.5 MeV.

1. Introduction

Scintillators are a type of phosphor that absorbs ionizing radiation and converts it into low-energy photons, and they are used to detect ionizing radiation when coupled with photodetectors.[1,2] Such scintillation detectors are widely utilized in various fields, including security,[3] medicine,[4] environmental measurements,[5] and astrophysics.[6] The required properties of scintillators vary depending on each application. For instance, a high scintillation light yield (*LY*), an emission wavelength suitable for photodetectors, high density and effective atomic number (Z_{eff}), and excellent chemical stability are often demanded.[7]

Most conventional scintillators have been developed in the form of single crystals.[8,9] Single crystals possess excellent optical properties and high uniformity, and they can be fabricated as large bulk materials. However, their fabrication generally requires long growth times and high production costs, and it is often difficult to grow materials owing to high melting points or phase transitions. Therefore, the development of scintillators in other material forms, such as transparent ceramics and glasses, has been actively investigated.[7,10–12] Among them, transparent ceramics have advantages such as a relatively short synthesis time, low-cost production, and high mechanical strength, since they are fabricated through solid-state reactions

*Corresponding author: e-mail: saito.yuma.sx6@naist.ac.jp
https://doi.org/10.18494/SAM6023

ISSN 0914-4935
https://myukk.org/

similar to those used for conventional opaque ceramics.[13] Moreover, transparent ceramics are particularly effective for materials with high melting points or phase transitions near the melting temperature.[14,15] To date, extensive studies on transparent ceramics have mainly focused on rare-earth sesquioxide and garnet-based materials.[13,16–19]

In this paper, we focused on Tm:Y_2O_3 transparent ceramics as scintillators. Y_2O_3 is a promising scintillator host because of its relatively high density (5.01 g/cm^3), high Z_{eff} (~37), and excellent chemical stability.[20–22] It also has a high melting point (2410 °C) and undergoes a phase transition at around 2270 °C,[23] making it suitable for fabrication in the transparent ceramic form.[24] As a luminescence center, Tm^{3+} exhibits sharp emission peaks in the range of 300–650 nm,[25,26] which matches the high-sensitivity region of conventional photodetectors. Although Tm:Y_2O_3 transparent ceramic scintillators have been fabricated,[16,27] their dependence on Tm concentration has not yet been systematically investigated. In this study, Tm:Y_2O_3 transparent ceramics with different Tm concentrations were prepared by the spark plasma sintering (SPS) method, and their optical and scintillation properties were examined.

2. Experimental Methods

Four Tm:Y_2O_3 transparent ceramic samples with Tm concentrations of 0.01, 0.1, 1.0, and 10 mol% were prepared by the SPS method. Tm_2O_3 (>99.99%, Furuuchi Chemical) and Y_2O_3 (>99.99%, Furuuchi Chemical) powders were used as starting materials, with a total weight of 0.6 g. The powders were mixed uniformly using a mortar and pestle, and the mixture enclosed in graphite punches and a die was then inserted into an SPS device (Sinter Land, LABOX-100). The sintering temperature was raised to 600 °C within 5 min and held for 5 min, then raised to 1400 °C within 8 min and maintained for 60 min under an applied pressure of 59 MPa. The samples were polished to a thickness of 1.0 mm using a polishing machine (MetaServ 250, BUEHLER).

Diffuse transmittance spectra and photoluminescence (PL) emission/excitation spectra were measured using a spectrometer (SolidSpec-3700, Shimadzu) and a spectrofluorometer (JASCO, FP-8600), respectively. X-ray-induced scintillation spectra,[18] decay curves,[28] afterglow profiles,[28] and pulse height spectra (PHS)[18] were measured using our original setup. Scintillation *LY*s of the Tm:Y_2O_3 samples were estimated by comparison with that of a commercial Ce:Gd_2SiO_5 (7000 photons/MeV, Hitachi Chemical). The shaping time was set to 10 μs, and the wavelength-dependent quantum efficiency of the photomultiplier tube (R7600-200) corresponding to the emission spectrum of each sample was calculated to be 35% (0.01% Tm), 32% (0.1% Tm), 31% (1.0% Tm), 32% (10% Tm), and 33% (Ce:Gd_2SiO_5).[29]

3. Results and Discussion

Figure 1 shows the diffuse transmittance spectra and the appearance of the Tm:Y_2O_3 transparent ceramic samples. The 0.01, 0.1, and 1.0% Tm samples exhibited transmittance above 50% in the visible wavelength range. Several absorption peaks were observed at approximately 360, 470, 660, 680, and 790 nm, which were attributed to the 4f–4f transitions of Tm^{3+}.[26] Figure 2 presents the PL excitation/emission spectra of the Tm:Y_2O_3 transparent ceramics. Excitation

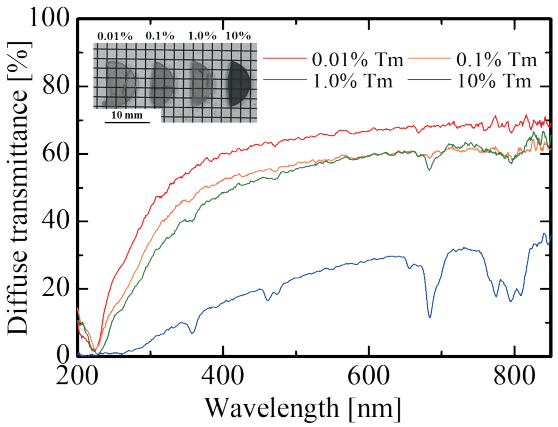

Fig. 1. (Color online) Diffuse transmittance spectra and picture (inset) of Tm:Y_2O_3 transparent ceramics.

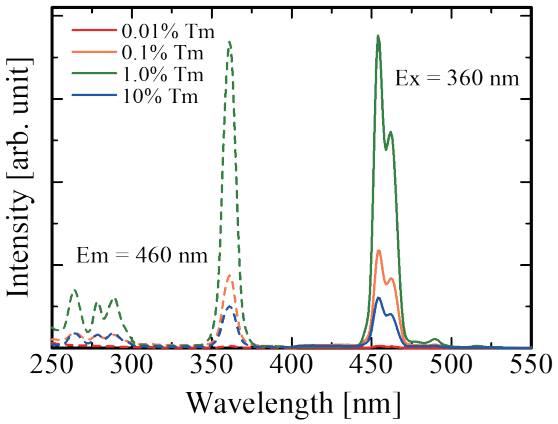

Fig. 2. (Color online) PL emission (solid) and excitation (dash) spectra.

peaks observed in the range of 250–360 nm correspond to the $^3H_6$–$^3P_{0,2}$ and $^1D_2$ transitions of Tm^{3+}.[30] Emission peaks at 460 and 480 nm are attributed to the $^1D_2$–$^3F_4$ and $^1G_4$–$^3H_6$ transitions of Tm^{3+}, respectively.[26] A pronounced decrease in the PL intensity observed for the 10% Tm sample can be ascribed to concentration quenching.

The X-ray-induced scintillation spectra are shown in Fig. 3. Emission bands can be classified into two features: a broad band appearing at 300–500 nm and several sharp peaks detected at 300–650 nm. The former band is attributed to the radiative recombination of self-trapped excitons (STE) of the Y_2O_3 host,[31] and its intensity decreased owing to Tm doping. The latter peaks originated from multiple 4f–4f transitions of Tm^{3+}, whose emission was quenched in the 10% Tm sample. Figure 4 indicates the X-ray-induced scintillation decay curves. The decay curves were approximated with a sum of two exponential components after excluding the instrumental response function. The origin of the τ_1 component can be ascribed to a marginal emission of the host and Tm^{3+}.[30] At low Tm concentrations (0.01–1.0%), the STE-related luminescence diminishes with increasing Tm, and τ_1 becomes increasingly dominated by the 4f–4f transitions of Tm^{3+}, resulting in the gradual increase in τ_1. In addition, the huge decrease in τ_1 for the 10% Tm sample is attributed to concentration quenching. The origin of τ_2 is assigned to the 4f–4f transitions of Tm^{3+}.[25,26,30] The longest τ_2 observed for the 0.01% Tm sample is attributed to the relatively low probability of nonradiative transitions among Tm^{3+} ions. At this low doping level, the average distance between Tm^{3+} ions is large, which suppresses cross-relaxation and energy migration processes, resulting in a longer decay time despite the weak overall Tm^{3+} luminescence. With increasing Tm concentration, the average distance between Tm^{3+} ions decreases, facilitating nonradiative energy transfer and thereby reducing τ_2. The huge decrease in τ_2 for the 10% Tm sample is, similarly to τ_1, attributed to concentration quenching.

Figure 5 shows the afterglow profiles. The evaluation methodology was the same as in our previous paper.[32] The afterglow ranged from approximately 250 to 800 ppm and tended to decrease with increasing Tm concentration. The 10% Tm-doped sample showed the lowest afterglow, which was close to that of the commercial Tl:CsI (268 ppm) scintillator evaluated under the same conditions.[28,33] Figure 6 presents the PHS of the Tm:Y_2O_3 transparent ceramics

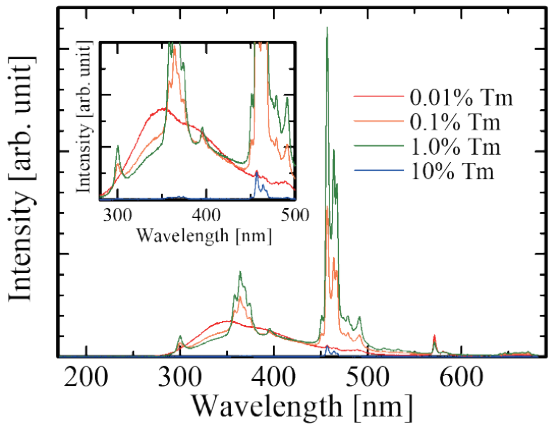

Fig. 3. (Color online) X-ray-induced scintillation spectra of Tm:Y_2O_3 transparent ceramics.

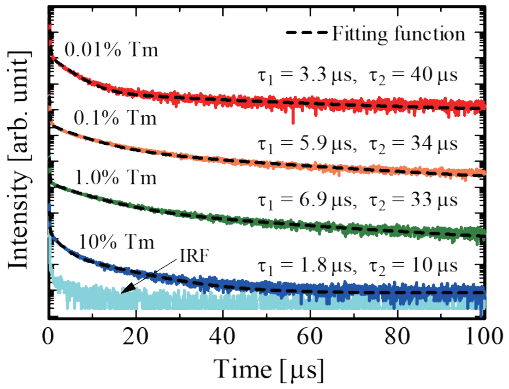

Fig. 4. (Color online) X-ray-induced scintillation decay curves of Tm:Y_2O_3 transparent ceramics.

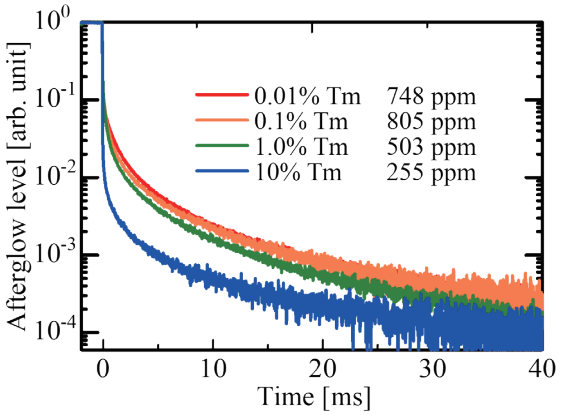

Fig. 5. (Color online) Afterglow profiles of Tm:Y_2O_3 transparent ceramics.

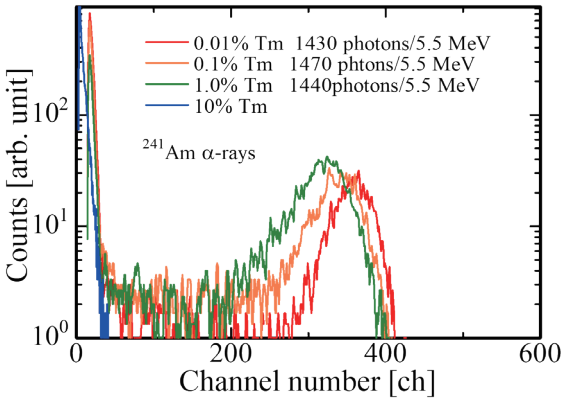

Fig. 6. (Color online) PHS of Tm:Y_2O_3 transparent ceramics under 241Am α-ray irradiation (5.5 MeV).

under ^{241}Am α-ray (5.5 MeV) irradiation. Distinct full-energy absorption peaks were observed for the 0.01, 0.1, and 1.0% Tm samples. The calculated *LY*s were 1430, 1470, and 1440 photons/5.5 MeV, respectively. This value was comparable to that previously reported for 0.15 mol% Tm:Y_2O_3 transparent ceramics (935–1400 photons/5.5 MeV).[16] The *LY* values of the 0.01–1.0% Tm samples remained almost constant, and no concentration dependence was observed. This is possibly due to a trade-off relationship of Tm^{3+}- and STE-related luminescence contributing to the overall *LY*. Another possibility is that the shaping time of 10 μs is insufficient to accumulate all the scintillation photons, and the estimated *LY* is underestimated in the highly Tm-doped samples.

4. Conclusions

Tm-doped Y_2O_3 transparent ceramics were successfully synthesized by the SPS method, and both PL and scintillation peaks appeared in the range of 350–650 nm, corresponding to the 4f–4f transitions of Tm^{3+}. The scintillation decay curves were well approximated by the sum of two

exponential components, with decay time constants of 1.8–6.9 and 10–40 μs. The scintillation *LY*s were estimated to be in the range of 1400–1500 photons/5.5 MeV.

Acknowledgments

This work was supported by JSPS KAKENHI (22H00309, 23K25126, 24K03197, 23K13689, and 25K08266), the Cooperative Research Project of the Research Center for Biomedical Engineering, Nippon Sheet Glass Foundation, and Hosokawa Powder Technology Foundation.

References

1 K. Watanabe: Jpn. J. Appl. Phys. **62** (2023) 010507. https://doi.org/10.35848/1347-4065/ac90a5
2 N. Kawaguchi, T. Kato, D. Nakauchi, and T. Yanagida: Jpn. J. Appl. Phys. **62** (2023) 010611. https://doi.org/10.35848/1347-4065/ac99c3
3 J. Glodo, Y. Wang, R. Shawgo, C. Brecher, R. H. Hawrami, J. Tower, and K. S. Shah: Phys. Procedia **90** (2017) 285. https://doi.org/10.1016/j.phpro.2017.09.012
4 C. W. E. van Eijk: Nucl. Instrum. Methods Phys. Res. A **509** (2003) 17. https://doi.org/10.1016/S0168-9002(03)01542-0
5 K. Watanabe, T. Yanagida, K. Fukuda, A. Koike, T. Aoki, and A. Uritani: Sens. Mater. **27** (2015) 269. https://doi.org/10.18494/SAM.2015.1093
6 M. Kole, M. Chauvin, Y. Fukazawa, K. Fukuda, S. Ishizu, M. Jackson, T. Kamae, N. Kawaguchi, T. Kawano, M. Kiss, E. Moretti, M. Pearce, S. Rydström, H. Takahashi, and T. Yanagida: Nucl. Instrum. Methods Phys. Res. A. **770** (2015) 68. https://doi.org/10.1016/j.nima.2014.10.016
7 C. Greskovich and S. Duclos: Annu. Rev. Mater. Sci. **27** (1997) 69. https://doi.org/10.1146/annurev.matsci.27.1.69
8 T. Yanagida, T. Kato, D. Nakauchi, and N. Kawaguchi: Jpn. J. Appl. Phys. **62** (2023) 010508. https://doi.org/10.35848/1347-4065/ac9026
9 Y. Fujimoto, M. Koshimizu, T. Yanagida, G. Okada, K. Saeki, and K. Asai: Jpn. J. Appl. Phys. **55** (2016) 090301. https://doi.org/10.7567/JJAP.55.090301
10 T. Kato, D. Nakauchi, N. Kawaguchi, and T. Yanagida: Sens. Mater. **36** (2024) 531. https://doi.org/10.18494/SAM4749
11 K. Miyajima, A. Nishikawa, T. Kato, D. Nakauchi, N. Kawaguchi, and T. Yanagida: Sens. Mater. **37** (2025) 481. https://doi.org/10.18494/SAM5436
12 K. Shinozaki, G. Okada, N. Kawaguchi, and T. Yanagida: Jpn. J. Appl. Phys. **62** (2023) 010603. https://doi.org/10.35848/1347-4065/ac95e6
13 Z. M. Seeley, N. J. Cherepy, and S. A. Payne: J. Mater. Res. **29** (2014) 2332. https://doi.org/10.1557/jmr.2014.235
14 W. Lou, Y. Tang, H. Chen, Y. Lei, H. Lin, R. Hong, Z. Han, and D. Zhang: J. Am. Ceram. Soc. **108** (2025) e20303. https://doi.org/10.1111/jace.20303
15 J. Zhang, L. An, M. Liu, S. Shimai, and S. Wang: J. Eur. Ceram. Soc. **29** (2009) 305. https://doi.org/10.1016/j.jeurceramsoc.2008.03.006
16 Y. Fujimoto, T. Yanagida, Y. Yokota, A. Ikesue, and A. Yoshikawa: Opt. Mater. **34** (2011) 448. https://doi.org/10.1016/j.optmat.2011.03.049
17 Y. Futami, T. Yanagida, Y. Fujimoto, J. Pejchal, M. Sugiyama, S. Kurosawa, Y. Yokota, A. Ito, A. Yoshikawa, and T. Goto: Radiat. Meas. **55** (2013) 136. https://doi.org/10.1016/j.radmeas.2013.01.014
18 T. Yanagida, K. Kamada, Y. Fujimoto, H. Yagi, and T. Yanagitani: Opt. Mater. **35** (2013) 2480. https://doi.org/10.1016/j.optmat.2013.07.002
19 H. Takahashi, T. Yanagida, D. Kasama, T. Ito, M. Kokubun, K. Makishima, T. Yanagitani, H. Yagi, T. Shigeta, and T. Ito: IEEE. Trans. Nucl. Sci. **53** (2006) 2404. https://doi.org/10.1109/TNS.2006.878575
20 E. Hasabeldaim, H. C. Swart, and R. E. Kroon: Physica B: Condens. Matter. **671** (2023) 415417. https://doi.org/10.1016/j.physb.2023.415417
21 T. Tomiki, J. Tamashiro, Y. Tanahara, A. Yamada, H. Fukutani, T. Miyahara, H. Kato, S. Shin, and M. Ishigame: J. Phys. Soc. Jpn. **55** (1986) 4543. https://doi.org/10.1143/JPSJ.55.4543
22 G. Skandan, C. M. Foster, H. Frase, M. N. Ali, J. C. Parker, and H. Hahn: Nanostruct. Mater. **1** (1992) 313. https://doi.org/10.1016/0965-9773(92)90038-Y
23 Y. Tskuda and A. Muta: JCS-Japan **84** (1976) 585. https://doi.org/10.2109/jcersj1950.84.976_585

24 A. Fukabori, T. Yanagida, J. Pejchal, S. Maeo, Y. Yokota, A. Yoshikawa, T. Ikegami, F. Moretti, and K. Kamada: J. Appl. Phys. **107** (2010) 073501. https://doi.org/10.1063/1.3330407
25 T. Kunikata, P. Kantuptim, D. Shiratori, T. Kato, D. Nakauchi, N. Kawaguchi, and T. Yanagida: Sens. Mater. **36** (2024) 457. https://doi.org/10.18494/SAM4754
26 K. Okazaki, D. Nakauchi, A. Nishikawa, T. Kato, N. Kawaguchi, and T. Yanagida: Sens. Mater. **36** (2024) 587. https://doi.org/10.18494/SAM4753
27 M. G. Chapman, M. R. Marchewka, S. A. Roberts, J. M. Schmitt, C. McMillen, C. J. Kucera, T. A. DeVol, J. Ballato, and L. G. Jacobsohn: J. Lumin. **165** (2015) 56. https://doi.org/10.1016/j.jlumin.2015.03.041
28 T. Yanagida, Y. Fujimoto, T. Ito, K. Uchiyama, and K. Mori: Appl. Phys. Express **7** (2014) 062401. https://doi.org/10.7567/APEX.7.062401
29 Y. Endo, K. Ichiba, D. Nakauchi, H. Fukushima, K. Watanabe, T. Kato, N. Kawaguchi, and T. Yanagida: Solid State Sci. **145** (2023) 107333. https://doi.org/10.1016/j.solidstatesciences.2023.107333
30 Y. Fujimoto, M. Sugiyama, T. Yanagida, S. Wakahara, S. Suzuki, S. Kurosawa, V. Chani, and A. Yoshikawa: Opt. Mater. **35** (2013) 2023. https://doi.org/10.1016/j.optmat.2012.10.010
31 Y. Futami, T. Yanagida, Y. Fujimoto, J. Pejchal, M. Sugiyama, S. Kurosawa, Y. Yokota, A. Ito, A. Yoshikawa, and T. Goto: Radiat. Meas. **55** (2013) 136. https://doi.org/10.1016/j.radmeas.2013.01.014
32 H. Fukushima, M. Akatsuka, H. Kimura, D. Onoda, D. Shiratori, D. Nakauchi, T. Kato, N. Kawaguchi, and T. Yanagida: Sens. Mater. **33** (2021) 2235. https://doi.org/10.18494/SAM.2021.3324
33 D. Nakauchi, T. Kato, N. Kawaguchi, and T. Yanagida: Appl. Phys. Express **13** (2020) 122001. https://doi.org/10.35848/1882-0786/abc574